



This is a repository copy of *Restoration of auditory evoked responses by human ES-cell-derived otic progenitors*.

White Rose Research Online URL for this paper:
<http://eprints.whiterose.ac.uk/108187/>

Version: Accepted Version

Article:

Chen, W., Jongkamonwiwat, N., Abbas, L. et al. (9 more authors) (2012) Restoration of auditory evoked responses by human ES-cell-derived otic progenitors. *Nature*, 490 (7419). pp. 278-282. ISSN 0028-0836

<https://doi.org/10.1038/nature11415>

Reuse

Unless indicated otherwise, fulltext items are protected by copyright with all rights reserved. The copyright exception in section 29 of the Copyright, Designs and Patents Act 1988 allows the making of a single copy solely for the purpose of non-commercial research or private study within the limits of fair dealing. The publisher or other rights-holder may allow further reproduction and re-use of this version - refer to the White Rose Research Online record for this item. Where records identify the publisher as the copyright holder, users can verify any specific terms of use on the publisher's website.

Takedown

If you consider content in White Rose Research Online to be in breach of UK law, please notify us by emailing eprints@whiterose.ac.uk including the URL of the record and the reason for the withdrawal request.



eprints@whiterose.ac.uk
<https://eprints.whiterose.ac.uk/>

Published in final edited form as:

Nature. 2012 October 11; 490(7419): 278–282. doi:10.1038/nature11415.

Restoration of auditory evoked responses by human ES cell-derived otic progenitors

Wei Chen^{1,2,*}, Nopporn Jongkamonwiwat^{1,2,4,*}, Leila Abbas^{1,2}, Sarah Jacob Eshtan^{1,2}, Stuart L. Johnson², Stephanie Kuhn², Marta Milo², Johanna K. Thurlow^{1,2}, Peter W. Andrews^{1,2}, Walter Marcotti², Harry D. Moore^{1,2}, and Marcelo N. Rivolta^{1,2,3}

¹Centre for Stem Cell Biology, University of Sheffield, Sheffield S10 2TN, United Kingdom

²Department of Biomedical Sciences, University of Sheffield, Sheffield S10 2TN, United Kingdom

⁴Faculty of Health Sciences, Srinakharinwirot University, Ongkharak, Nakhonnayok 26120, Thailand

Abstract

Deafness is a condition with a high prevalence worldwide, produced primarily by the loss of the sensory hair cells and their associated spiral ganglion neurons (SGNs). Of all the forms of deafness, auditory neuropathy is of a particular concern. This condition, defined primarily by damage to the SGNs with relative preservation of the hair cells¹, is responsible for a substantial proportion of patients with hearing impairment². While the loss of hair cells can be circumvented partially by a cochlear implant, no routine treatment is available for sensory neuron loss since poor innervation limits the prospective performance of an implant³. Using stem cells to recover the damaged sensory circuitry is a potential therapeutic strategy. Here, we present a protocol to induce differentiation from human embryonic stem cells (hESCs) using signals involved in the initial specification of the otic placode. We obtained two types of otic progenitors able to differentiate *in vitro* into hair cell-like cells and auditory neurons that display expected electrophysiological properties. Moreover, when transplanted into an auditory neuropathy model, otic neuroprogenitors engraft, differentiate and significantly improve auditory evoked response (ABR) thresholds. These results should stimulate further research into the development of a cell-based therapy for deafness.

Hair cell-like phenotypes and sensory neurons, with different degrees of functional maturation, have been obtained from mouse stem populations⁴⁻¹⁰. After transplantation, some cell types have showed engraftment but none have demonstrated evidence of functional recovery¹⁰⁻¹⁵. Although useful for research purposes, these products are unsuitable for a therapeutic application and to date appropriate cell types of human origin have remained elusive. Neuroprogenitors isolated from mature human cochleae display limited proliferative and differentiating potential¹⁶ while hESCs-derived neural crest cells

Correspondence should be addressed to M.N.R. (m.n.rivolta@sheffield.ac.uk).. ³Corresponding author: Centre for Stem Cell Biology and Department of Biomedical Sciences, University of Sheffield, Alfred Denny Building, Western Bank, Sheffield S10 2TN, UK
Phone: 44 (0) 114 2222385 Fax: 44 (0) 114 222 2787 m.n.rivolta@sheffield.ac.uk.

*These authors contributed equally to this work.

Supplementary Information, Methods and Spreadsheets are linked to the online version of the paper.

Author Contributions W.C., N.J., L.A., S.J.E and J.K.T: Collection and/or assembly of data, data analysis and interpretation; S.L.J., S.K. and W.M.: Collection and/or assembly of electrophysiology data, its analysis and interpretation; M.M.: Biocomputational analysis of gene array data; P.W.A. and H.D.M.: provision of study material, administrative support; M.N.R: Conception and design, financial support, collection and/or assembly of data, its analysis and interpretation, manuscript writing, final approval of manuscript.

Author information Microarray datasets have been deposited at the NCBI Gene Expression Omnibus and they can be retrieved with accession number GSE36754. The authors declare no competing financial interest.

may differentiate into sensory neurons by exposure to BMP but lack true otic characteristics^{17,18}. Recently, we isolated a population of bipotent stem cells from the human fetal cochlea (hFASCs), with the ability to produce hair cell-like cells and neurons¹⁹. However, although hFASCs can be expanded *in vitro* for ~25 population doublings, they eventually undergo replicative senescence. Hence, there is a need for a reliable, renewable source of human otic progenitors, with the ability to produce both cell types for sensory replacement.

FGF signaling is necessary and sufficient for the induction *in vivo* of the otic placode, the primordium of the hearing organ^{20,21}. Since in the mouse the ligands involved in placode signaling have been identified as FGF3 and FGF10^{22,23}, we hypothesized that exposure to these factors would trigger otic differentiation of hESCs. Initial experiments with embryoid bodies (EBs) confirmed FGF3 and 10 induction of otic features (Supplementary Fig. 1a) therefore we focused on developing a method devoid of this initial cell-aggregation step, which is prone to high variability. Undifferentiated colonies of hESCs were dissociated for plating as a monolayer on laminin-coated flasks (see Supplementary Methods). Under these conditions, FGF3+10 treatment induced the placodal markers *PAX8* and *PAX2*, either in the presence of KOSR or under defined conditions using DFNB medium (Supplementary Methods, Supplementary Figs. 1b-2). Global analyses of gene expression was performed using Affymetrix GeneChip arrays and, after normalization (see Supplementary Methods), samples were mined in two different ways. In the first we used the Gene Set Enrichment Analysis (GSEA) tool²⁴ to look for genes that were enriched in the entire list of probe sets, without establishing a priori cut off of differential expression (Supplementary Table 1-2). This analysis showed that a set of otic markers was significantly enriched in the FGF-treated samples when compared with the undifferentiated hESCs (normalized enriched score, NES: 0.568, family-wise error rate *p*-value, FWER*p* 0.046) or cells grown in DFNB (NES: 0.707, FWER*p* 0.019) (Supplementary Table 1). A second type of analysis assessed genes differentially expressed using predefined criteria for fold change cut off and statistical significance (see Supplementary Methods). A total of 1,424 genes (represented by 2,124 probe sets) was differentially upregulated in the FGF-samples when compared to undifferentiated hESCs, while 423 genes (505 probe sets) were upregulated in the FGF-treated vs. the DFNB controls (Supplementary spreadsheets 1-2). On the other hand, 2,368 genes (3,231 probe sets) were downregulated in the FGF-samples vs hESCs and 482 genes (607 probe sets) were downregulated vs DFNB (Supplementary spreadsheets 3-4). In a gene ontology (GO) analysis, the GO terms 'sensory organ development' (EASE *p*-value score in FGF vs hESC: 3.92×10^{-15} ; FGF vs DFNB: 0.022); 'ear development' (FGF vs hESC: 4.47×10^{-8} ; FGF vs DFNB: 0.014) and 'ear morphogenesis' (FGF vs hESC: 3.08×10^{-6} ; FGF vs DFNB: 0.0497) were highly enriched in the FGF-treated cells in both comparisons, while 'mechanoreceptor differentiation' and 'auditory receptor differentiation' were up in FGF vs hESC (See Supplementary Spreadsheets 5-8). Both bioinformatics analyses therefore suggested that the FGF treatment was generating a global change of transcription compatible with the induction of otic progenitors.

We also used immunostaining to examine the co-expression of *PAX8* and *SOX2*, to define the otic progenitors at a cellular level. Otic progenitors grew as colonies after the inductive phase. Initial immunolabelling showed a relatively large proportion of double positive cells in the FGF-treated condition (~78%), in contrast to the relatively moderate upregulation of otic transcripts detected with the arrays. However, a subset of cells expressed very high levels of *PAX8* and *SOX2*, and these were assessed with an automated microscopy platform (InCell Analyzer 1000) that enabled quantification of the number of positive cells and their relative intensity (Fig. 1 and Supplementary Figure 3). When a stringent threshold was selected (75th intensity percentile per cell line and antibody, see Supplementary Methods) 18.3%±0.8 of the cells expressed high levels of *PAX8* and *SOX2* (*PAX8*^{hi}*SOX2*^{hi}) after

FGF treatment (against 0% obtained without the growth factors, $p < 0.001$) while $18\% \pm 2$ cells were PAX8^{hi}/FOXG1^{hi} (compared to $4\% \pm 4$ obtained in the control, $p < 0.001$). PAX8^{hi}SOX2^{hi}FOXG1^{hi} cells also expressed the otic markers PAX2, NESTIN, SIX1 and GATA3 (Fig. 2h and Supplementary Figs. 4-5a). It is likely that this subset of PAX8^{hi}SOX2^{hi}FOXG1^{hi} expressing cells represents the otic progenitors. The reproducibility of the protocol was tested across the hESC lines H7, H14 and Shef3, which all gave comparable results (see Fig. 1 and Supplementary Figure 3). FGF3 and 10 induced two morphologically distinct types of otic colonies (Fig. 2a-h). One cell population showed a flat phenotype, with large cytoplasm and formed epithelioid islands (Fig. 2a-d), while the second was small, with denser chromatin and presented cytoplasmic projections (Fig. 2e-f). Given their morphological appearance we have operationally named them otic epithelial progenitor (OEP) and otic neural progenitor (ONP), respectively. The relative proportion of these progenitors was dependent on the cell line, plating density and the degree of cell separation (single cells versus cell clusters) (Supplementary Figs. 5-6 and Supplementary Methods). Progenitor colonies were purified using sequential dissociation (see Supplementary Methods), yielding moderately homogenous cultures of the desired cell colony type and were expanded in OSCFM (Otic stem cell full media, Suppl. Methods).

The differentiation potential of OEPs and ONPs was tested in ‘neuralizing’ and ‘hair cell’ culture conditions developed previously using hFASCs¹⁹ (see Supplementary Methods). OEPs produced hair cell-like cells as defined by the simultaneous expression of ATOH1 and BRN3C, or BRN3C and MYO7A (~45%) (Supplementary Fig. 7). A small subset differentiated a rudimentary apical bundle, expressing ESPIN (Supplementary Fig 8). These hair cell-like cells also expressed an outward K⁺ current, the inward rectifier K⁺ current I_{K1} and an inward Ca²⁺ current (I_{Ca}) (Supplementary Fig. 9). Under ‘neuralizing’ conditions, they produced a small proportion (~9%) of sensory neurons (Supplementary Fig 7). On the other hand, ONPs were committed to produce neurons. Under ‘neuralizing’ conditions, almost all cells developed a bipolar morphology and were positive for BRN3A and β -tubulinIII, as well as for β -tubulinIII and NF200. They also expressed *NEUROD1*, *ISLET-1* and *TrkB*, a delayed-rectifier K⁺ current (I_K), a Na⁺ current (I_{Na}), and elicited single action potentials (Supplementary Fig. 9). No hair cell differentiation was obtained from ONPs under ‘neuralizing’ or ‘hair cell’ culture conditions. Detailed results are given in Supplementary Information.

The properties of ONPs *in vivo* were studied by transplanting them into ouabain-treated gerbils, a model of neuropathic deafness²⁵. Application of ouabain directly to the round window selectively damages the type I SGNs, preserving the hair cells and the organ of Corti²⁶ (Supplementary Fig. 10). After ouabain application, only a small number of SGNs survived (6.4%, see Supplementary Table 3). Most of the surviving cells (~87%) were peripherin+, type II neurons therefore less than 1% of the original population of type I neurons remained (Supplementary Table 3 and Supplementary Fig. 13). Staining for myosin VIIa and the presence of distortion product otoacoustic emissions (DPOAEs) confirmed that the organ of Corti had not been damaged (Supplementary Figs. 10 and 11). DPOAEs are sounds produced as a consequence of electromechanical feedback from the outer hair cells and can be used to check their physiological integrity.

ONPs derived from Shef1 hESCs constitutively expressing either eGFP or Tomato fluorescent protein were expanded in OSCFM, dissociated with trypsin and delivered directly into the modiolus, approaching the cochlea through the round window. One set of animals was transplanted 3-5 days after ouabain application ($n=13$) while another was transplanted two weeks after the ototoxic drug ($n=5$). Since no functional or histological differences were encountered between the two groups ($p > 0.05$; Supplementary Fig. 12), they were analyzed together. Two to three weeks after transplantation, five out of six animals had

surviving, transplanted cells grafted in the modiolus, forming an ectopic spiral ganglion (Fig. 3a-b). Cells in the marginal sides of the ectopic ganglion had undergone differentiation as judged by β -tubulin III staining (Fig. 3b) and displayed neural projections, targeting the organ of Corti (Fig. 3c-d). Animals were then followed up for 10 weeks posttransplantation (PT). Histological analysis after 10 weeks PT showed that the ectopic ganglion was still present and cells had also migrated into the Rosenthal's canal (Fig. 3e). Transplanted cells expressed the 3A10 neurofilament-associated antigen and NKA α 3, a marker of type I neurons and afferent fibers in the inner ear²⁷ (Supplementary Fig. 14). Significantly, projections from the transplanted cells that reached the organ of Corti were targeting the hair cells, and fibers positive for NKA α 3 and GluA2 were observed next to the basal pole of the inner hair cells suggesting the presence of synaptic connections (Fig. 3g). Moreover, fibers from the transplanted cells were visualized leaving the modiolus towards the brainstem (Fig. 3f). In the cochlear nucleus of three gerbils we found RFP-positive fibers also stained for synaptophysin, suggesting synaptic connections with the central auditory path (Fig. 3h-i). Transplanted ONPs contributed significantly to restore neuronal density (Fig. 3j, $p < 0.01$). While 112.5 ± 11.9 TuJ1⁺ mm⁻² cells were present in the ouabain-treated, untransplanted ears, 546.4 ± 30.6 TuJ1⁺ mm⁻² were found after transplantation. From these, $94.9 \pm 0.3\%$ were also GFP (or Tomato) positive, confirming their exogenous nature (Supplementary Table 4). The number of projections detected in the brainstem was considerably lower than the number of transplanted cell bodies identified in the ganglion. While this could be explained by the limited sorting of fluorescent protein into the long afferent fibers, the pathfinding of the central innervations should require further future exploration. No tumors were detected in any of the transplanted animals at any stage throughout the experiment.

Functional performance was determined by measuring ABRs thresholds. These were established based on the wave ii-wave iii (P2-N3) amplitude²⁸. These waves are generated by the cochlear nucleus and the superior olivary complex cells, and reflect neural connections with the central auditory pathway²⁹. After ouabain application, auditory function was severely impaired, with thresholds rising from 20dB SPL to almost 80dB SPL, the maximum intensity tested. Frequency discrimination was also abolished. The amplitudes of wave ii-iii complexes were almost negligible at any of the frequencies explored at the maximum intensity of 80dB SPL (Fig. 4d). ABRs were recorded at 1-2 week intervals. Control animals ($n=8$) showed no sign of functional recovery throughout the experiment, with a mean auditory threshold after 10 weeks of 75.14 ± 2.3 dB; similar to the 76.37 ± 1.8 dB obtained after ouabain treatment. However in the transplanted animals ($n=18$), there was a detectable improvement in the ABR thresholds (Fig. 4a-b) starting approximately four weeks PT, with the mean auditory threshold lowered (improved) to 50.4 ± 4.5 dB by 10 weeks PT. Furthermore, the mean auditory threshold shift, calculated as the difference between the threshold at 10 weeks PT versus the one before ouabain treatment, was of 53 ± 1.7 dB in the control animals, compared to 28.6 ± 3.6 dB in the transplanted cohort ($p = 0.0002$, Fig. 4c). This represents an overall functional improvement of ~46%. The range of recovery went from modest to almost complete (see Supplementary Fig. 15), which is remarkable considering the technical challenges involved in the procedure. Tonotopical processing was also partially restored (Fig. 4d). A trend in the increment of wave ii-iii amplitudes was detected at each frequency explored, with amplitudes being significantly different at 22, 26 and 30 kHz, when compared to the untransplanted animals ($p < 0.05$). When compared to the amplitudes before the ouabain application, the improvement was ~43%. Latencies were mostly similar to the ones before ouabain (Fig. 4e). The only significant difference was detected at 30 kHz (BO: 4.58 ± 0.2 ms, $n=6$; PT: 5.9 ± 0.4 ms, $n=5$; $p < 0.05$) suggesting that some maturation was still taking place at this stage. Finally, there was a significant correlation between the increment of neural density by transplanted cells and the lowering of the ABR threshold ($R^2=0.3867$, $p < 0.05$, Fig. 4f).

Our developmentally-informed protocol produced hESC-derived auditory hair cells and neurons that closely resembled phenotypes obtained from hFASCs, providing validation of their cochlear characteristics. This was further supported by the restoration of ABR thresholds on transplantation of otic progenitors into a deaf adult mammal. The ability to reinstate auditory neuron functionality paves the way for a future cell-based treatment for auditory neuropathies. It may also, in combination with a cochlear implant, offer a therapeutic solution to a wider range of patients that currently remain without viable treatment.

Methods Summary

hESCs lines used (H7, H14, Shef1, Shef3, Shef1-EGFP and Shef1-Tomato), with a normal karyotype, were maintained on mouse embryonic fibroblast feeders (MEFs) under standard conditions. While EBs and initial monolayer experiments were performed in the presence of Knock Out Serum Replacement (KOSR), we later adopted a chemically-defined medium. This serum-free, chemically defined basal culture media included a 1:1 mixture of Dulbecco's Modified Eagle's Medium (DMEM):Ham's F12 and N2/B27 supplements (DFNB). In most experiments, FGF3 and FGF10 were used at 50ng ml⁻¹. Laminin (R&D Systems) was used at 5 µg cm⁻². Antibodies, PCR primers and microarray analysis are detailed in the supplementary methods. To induce hair cell differentiation, progenitors were transferred to gelatin-coated dishes and cultured with DFNB supplemented with all-*trans* retinoic acid (10⁻⁶ M, Sigma) and EGF (20ng/ml) for 2-4 weeks. To induce neuronal differentiation, cells dissociated with trypsin were plated on gelatin-coated dishes and incubated in DFNB with bFGF (20ng/ml) and Sonic Hedgehog (Shh-C24II, 500ng/ml, R&D Systems). On the third day, culture was supplemented with neurotrophin3 (NT-3, 10 ng/ml, Petropetch) and brain-derived neurotrophic factor (BDNF, 10 ng/ml, Petropetch). Shh-C24II was removed at the fourth-fifth day while the neurotrophins remained for the length of the incubation, normally between 7-14 days. Conditions for electrophysiological recordings are detailed in the supplementary methods. The auditory neuropathy model was generated by applying 1 mM ouabain directly into the RW niche of adult gerbils. Either three days or 2 weeks later, hONPs, expressing eGFP or Tomato fluorescent protein were injected into the modiolus. Functional recovery was monitored weekly by measuring ABRs and DPOAEs, for up to 10 weeks. Cochleae were taken, fixed and processed for analysis. Details for the hearing test and histological preparation are provided in the supplementary methods section.

Supplementary Material

Refer to Web version on PubMed Central for supplementary material.

Acknowledgments

This work was supported primarily by grants from Action on Hearing Loss (RNID) to M.N.R. Other support included Deafness Research UK (M.N.R, W.M.), Wellcome Trust (088719, W.M.), MRC (P.W.A, HDM, M.N.R) and ESTOOLS (P.W.A). S.L.J. was supported by a Wellcome Trust VIP award and the RNID. W.M. and S.L.J. are Royal Society University Research Fellows. Confocal images were taken at the Light Microscopy Facility of the Department of Biomedical Sciences. We are grateful for the advice by Dr. Mike Mulheran and Prof. Ian Russell on the tests of auditory function, provided at the earlier stages of this project and to the assistance of Dr. Paul Gokhale on the use of the InCell Analyzer. M.N.R. dedicates this work to the memory of his parents, Noemí Luján-Ceballos and Juan Carlos Rivilta.

References

1. Vlastarakos PV, Nikolopoulos TP, Tavoulari E, Papacharalambous G, Korres S. Auditory neuropathy: endocochlear lesion or temporal processing impairment? Implications for diagnosis and

- management. *International journal of pediatric otorhinolaryngology*. 2008; 72:1135–1150. [PubMed: 18502518]
2. Uus K, Bamford J. Effectiveness of population-based newborn hearing screening in England: ages of interventions and profile of cases. *Pediatrics*. 2006; 117:e887–893. [PubMed: 16651292]
 3. Bradley J, Beale T, Graham J, Bell M. Variable long-term outcomes from cochlear implantation in children with hypoplastic auditory nerves. *Cochlear implants international*. 2008; 9:34–60. [PubMed: 18246534]
 4. Li H, Liu H, Heller S. Pluripotent stem cells from the adult mouse inner ear. *Nat Med*. 2003; 9:1293–1299. [PubMed: 12949502]
 5. Li H, Roblin G, Liu H, Heller S. Generation of hair cells by stepwise differentiation of embryonic stem cells. *Proc Natl Acad Sci U S A*. 2003; 100:13495–13500. [PubMed: 14593207]
 6. Oshima K, et al. Mechanosensitive hair cell-like cells from embryonic and induced pluripotent stem cells. *Cell*. 2010; 141:704–716. [PubMed: 20478259]
 7. Jeon SJ, Oshima K, Heller S, Edge AS. Bone marrow mesenchymal stem cells are progenitors in vitro for inner ear hair cells. *Molecular and cellular neurosciences*. 2007; 34:59–68. [PubMed: 17113786]
 8. Kondo T, Johnson SA, Yoder MC, Romand R, Hashino E. Sonic hedgehog and retinoic acid synergistically promote sensory fate specification from bone marrow-derived pluripotent stem cells. *Proc Natl Acad Sci U S A*. 2005; 102:4789–4794. [PubMed: 15778294]
 9. Coleman B, Fallon JB, Pettingill LN, de Silva MG, Shepherd RK. Auditory hair cell explant co-cultures promote the differentiation of stem cells into bipolar neurons. *Exp Cell Res*. 2007; 313:232–243. [PubMed: 17112512]
 10. Reyes JH, et al. Glutamatergic neuronal differentiation of mouse embryonic stem cells after transient expression of neurogenin 1 and treatment with BDNF and GDNF: in vitro and in vivo studies. *J Neurosci*. 2008; 28:12622–12631. [PubMed: 19036956]
 11. Corrales CE, et al. Engraftment and differentiation of embryonic stem cell-derived neural progenitor cells in the cochlear nerve trunk: growth of processes into the organ of Corti. *J Neurobiol*. 2006; 66:1489–1500. [PubMed: 17013931]
 12. Hildebrand MS, et al. Survival of partially differentiated mouse embryonic stem cells in the scala media of the guinea pig cochlea. *J Assoc Res Otolaryngol*. 2005; 6:341–354. [PubMed: 16208453]
 13. Sekiya T, et al. Transplantation of conditionally immortal auditory neuroblasts to the auditory nerve. *Eur J Neurosci*. 2007; 25:2307–2318. [PubMed: 17445229]
 14. Lang H, et al. Transplantation of mouse embryonic stem cells into the cochlea of an auditory-neuropathy animal model: effects of timing after injury. *J Assoc Res Otolaryngol*. 2008; 9:225–240. [PubMed: 18449604]
 15. Hu Z, Ulfendahl M, Olivius NP. Central migration of neuronal tissue and embryonic stem cells following transplantation along the adult auditory nerve. *Brain Res*. 2004; 1026:68–73. [PubMed: 15476698]
 16. Rask-Andersen H, et al. Regeneration of human auditory nerve. In vitro/in vivo demonstration of neural progenitor cells in adult human and guinea pig spiral ganglion. *Hear Res*. 2005; 203:180–191. [PubMed: 15855043]
 17. Shi F, Corrales CE, Liberman MC, Edge AS. BMP4 induction of sensory neurons from human embryonic stem cells and reinnervation of sensory epithelium. *Eur J Neurosci*. 2007; 26:3016–3023. [PubMed: 18005071]
 18. Lee G, et al. Isolation and directed differentiation of neural crest stem cells derived from human embryonic stem cells. *Nature biotechnology*. 2007; 25:1468–1475.
 19. Chen W, et al. Human fetal auditory stem cells can be expanded in vitro and differentiate into functional auditory neurons and hair cell-like cells. *Stem Cells*. 2009; 27:1196–1204. [PubMed: 19418454]
 20. Martin K, Groves AK. Competence of cranial ectoderm to respond to Fgf signaling suggests a two-step model of otic placode induction. *Development*. 2006; 133:877–887. [PubMed: 16452090]
 21. Freter S, Muta Y, Mak SS, Rinkwitz S, Ladher RK. Progressive restriction of otic fate: the role of FGF and Wnt in resolving inner ear potential. *Development*. 2008; 135:3415–3424. [PubMed: 18799542]

22. Alvarez Y, et al. Requirements for FGF3 and FGF10 during inner ear formation. *Development*. 2003; 130:6329–6338. [PubMed: 14623822]
23. Wright TJ, Mansour SL. Fgf3 and Fgf10 are required for mouse otic placode induction. *Development*. 2003; 130:3379–3390. [PubMed: 12810586]
24. Subramanian A, et al. Gene set enrichment analysis: a knowledge-based approach for interpreting genome-wide expression profiles. *Proc Natl Acad Sci U S A*. 2005; 102:15545–15550. [PubMed: 16199517]
25. Schmiedt RA, Okamura HO, Lang H, Schulte BA. Ouabain application to the round window of the gerbil cochlea: a model of auditory neuropathy and apoptosis. *J Assoc Res Otolaryngol*. 2002; 3:223–233. [PubMed: 12382099]
26. Lang H, Schulte BA, Schmiedt RA. Ouabain induces apoptotic cell death in type I spiral ganglion neurons, but not type II neurons. *J Assoc Res Otolaryngol*. 2005; 6:63–74. [PubMed: 15735933]
27. McLean WJ, Smith KA, Glowatzki E, Pyott SJ. Distribution of the Na,K-ATPase alpha subunit in the rat spiral ganglion and organ of corti. *J Assoc Res Otolaryngol*. 2009; 10:37–49. [PubMed: 19082858]
28. Burkard R, Boettcher F, Voigt H, Mills J. Comments on “Stimulus dependencies of the gerbil brain-stem auditory-evoked response (BAER). I: Effects of click level, rate and polarity” [J. Acoust. Soc. Am. 85, 2514-2525 (1989)]. *The Journal of the Acoustical Society of America*. 1993; 94:2441–2442. [PubMed: 8227757]
29. Boettcher FA, Mills JH, Norton BL. Age-related changes in auditory evoked potentials of gerbils. I. Response amplitudes. *Hear Res*. 1993; 71:137–145. [PubMed: 8113132]

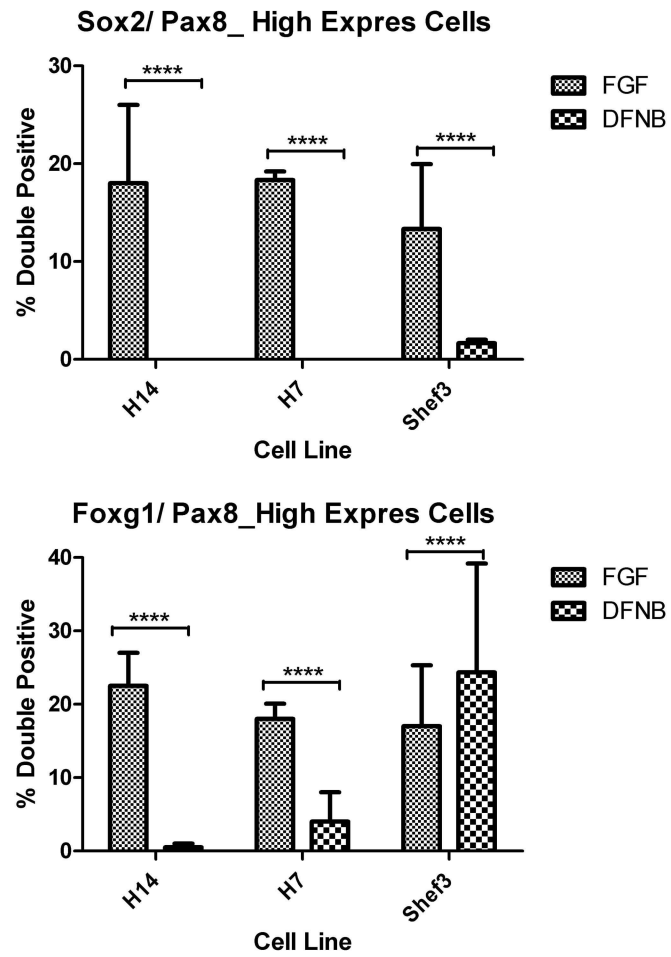


Figure 1. FGF3 and 10 generates otic progenitors

Bar chart showing the percentage of highly double positive cells at the FGF 75th percentile threshold ($n=3$; mean + s.e.m).

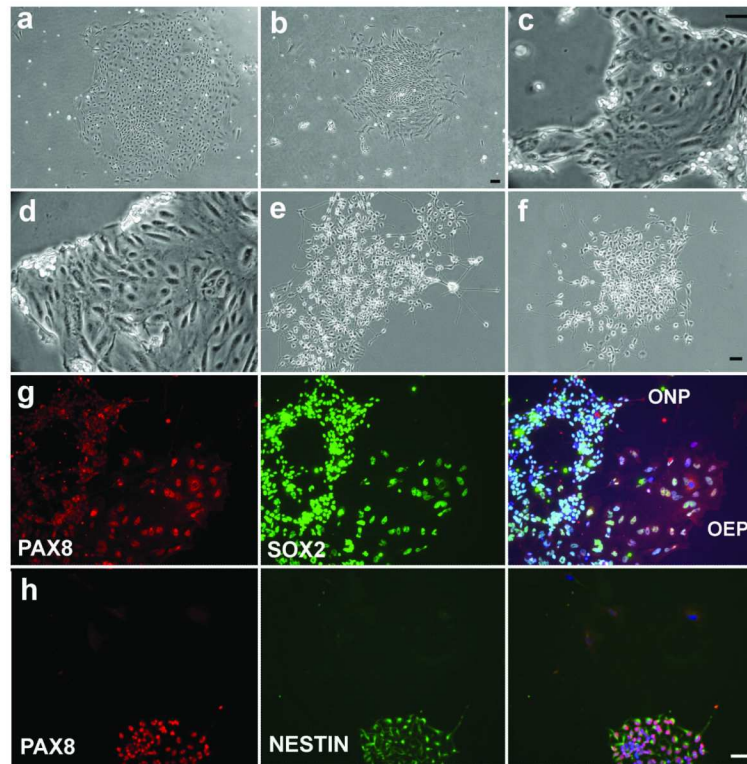


Figure 2. Otic epithelial (OEPs) and Otic Neuro progenitors (ONPs)

a and **b**. Morphology of an OEP colony. Bar is 100 μm . In all remaining panels, bar is 50 μm . **c** and **d**. Show the partial lifting of OEPs when treated with a short, mild trypsin incubation. **e** and **f**. Typical morphology of ONPs, showing cytoplasmic projections. **g**. Side-by-side ONP and OEP colonies, double-labeled for PAX8 and SOX2. **h**. ONP colony labeled for PAX8 and NESTIN.

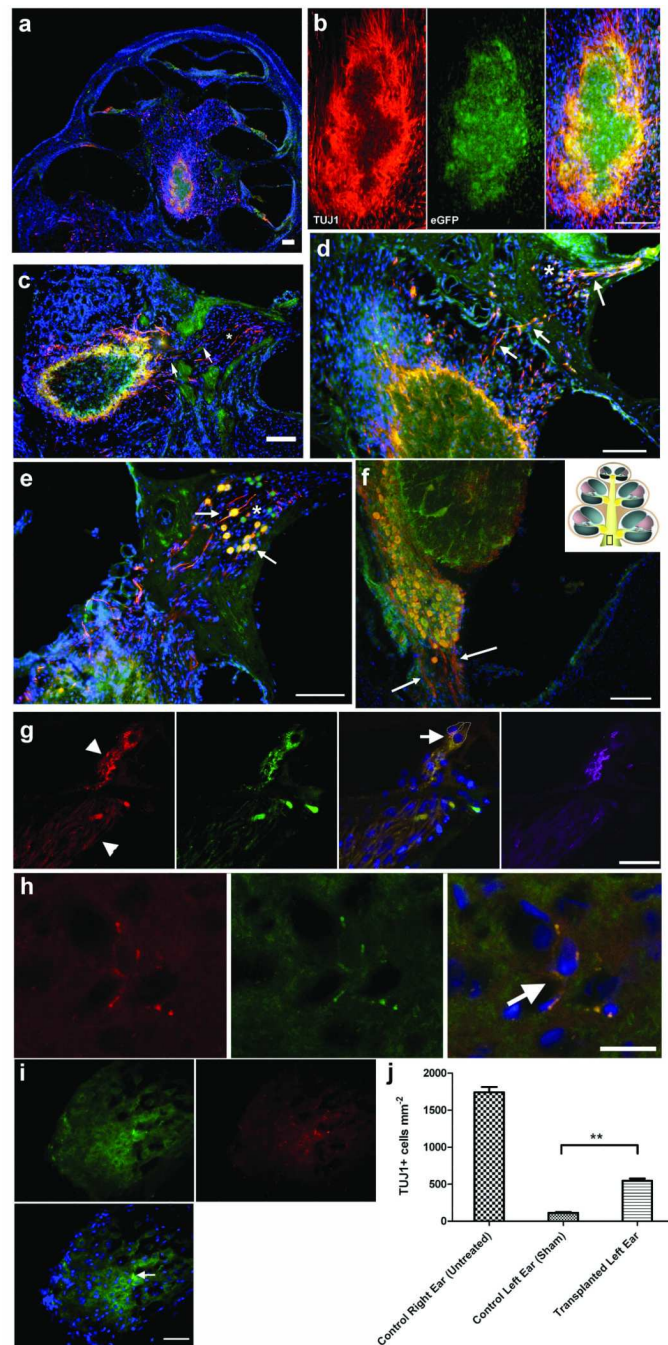


Figure 3. Transplantation of otic progenitors restores a population of spiral ganglion neurons
a. Mid-modiolar section of a transplanted cochlea showing the location of the newly formed, ectopic ganglion. **b.** Detail of the ganglion showing neuronal differentiation by TuJ1 staining (red). Neural fibers project from the ganglion towards the organ of Corti (**c** and **d**, arrows), passing through the Rosenthal's canal (**c** and **d**, asterisk). **e.** New neuronal bodies (arrows) are also found in the Rosenthal's canal (asterisk). **f.** Ectopic ganglion at the base of the modiolum, projecting TuJ1⁺ fibers centrally, towards the internal auditory meatus. **g.** RFP⁺ fibers (arrowheads) approaching the inner hair cells and expressing GluA2 (green), primarily concentrated in postsynaptic densities (PSDs) around the basal pole of IHCs

(arrow). Dotted lines show the positions of the IHCs. Fibers (including PSDs) were also positive for NKA α 3 (purple), a marker of afferent terminals. Nine out of ten animals analyzed had fibers contacting the IHC, while the three animals labeled for GluA2, were positive. **h, i.** RFP⁺ fibers in the cochlear nucleus, expressing synaptophysin (green, arrows). In (**h**), the fiber branches and surrounds the cell, with morphology highly reminiscent of the maturing endbulb of Held. **j.** SGN density 10 weeks after transplantation. Conditions compared are cochleae treated with ouabain and sham operated versus those with ouabain and transplanted with ONPs. Density was significantly increased ($p < 0.01$) from 112.5 ± 11.9 ($n=3$; mean + s.e.m) to 546.4 ± 30.6 ($n=8$). As a reference, the density of the control, untreated cochleae was $1,743 \pm 71.5$ TuJ1⁺ cells mm⁻². Scale bars for **a-f** are 100 μ m and for **g-i** are 50 μ m.

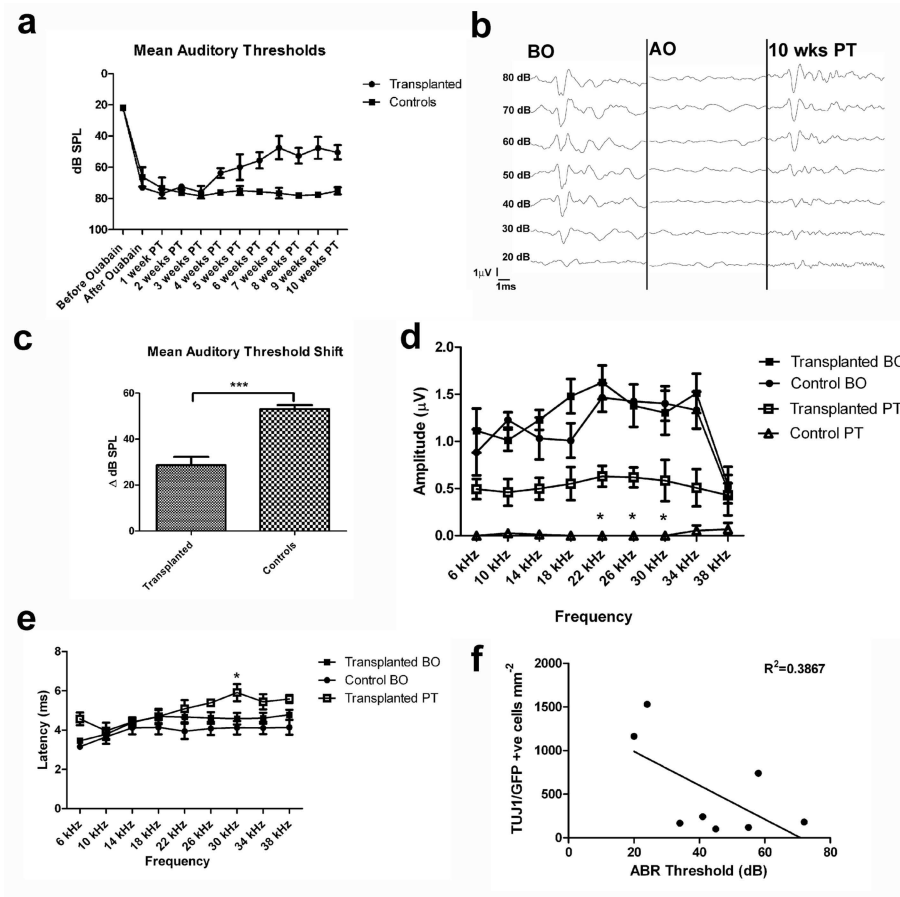


Figure 4. Transplanted cells provide a recovery of ABR thresholds

a. Evolution of the mean ABR thresholds (click) obtained in the transplanted animals ($n=18$; mean \pm s.e.m) compared to the controls ($n=8$). **b.** Trace ABR showing the abolition of waves after ouabain treatment (AO) and the restoration of the complexes 10 weeks posttransplantation (PT). **c.** Graph showing the mean auditory threshold shift reduction obtained by the transplantation (transplanted 28.6 ± 3.6 dB; $n=18$ vs 53 ± 1.7 dB; $n=8$ in the control, $p=0.0002$; mean \pm s.e.m). **d.** Comparison of the wave ii-iii amplitudes obtained by tone ABRs. A general trend of enhanced amplitudes was obtained across all frequencies tested, being significantly different from the untransplanted controls at 22, 26 and 30 kHz. Amplitudes before ouabain (BO) were equivalent between the transplanted ($n=6$) and untransplanted animals ($n=5$; mean \pm s.e.m). **e.** Latencies of wave ii-iii complexes were, in general, comparable before ouabain and after transplantation. Only at 30 kHz, a significant delay was observed (BO: 4.58 ± 0.2 ms, $n=6$; PT: 5.9 ± 0.4 ms, $n=5$; $p < 0.05$; mean \pm s.e.m). **f.** A significant correlation was observed between the mean density of TuJ1/GFP positive cells and the ABR thresholds ($n=8$; $p < 0.05$).